**FULL PAPER**

WILEY Applied Organometallic Chemistry

# Organoboron Schiff bases as cell-staining fluorescent probes: Synthesis, Chemio-photophysical characterization, DFT, and X-ray structures

Marisol Ibarra-Rodríguez[1] | Blanca M. Muñoz-Flores[1] (ID) | Alberto Gómez-Treviño[1] |

Rodrigo Chan-Navarro[1] | Jessica C. Berrones-Reyes[1] | Arturo Chávez-Reyes[2] |

H.V. Rasika Dias[3] (ID) | Mario Sánchez Vázquez[4] | Víctor M. Jiménez-Pérez[1] (ID)

[1] Universidad Autónoma de Nuevo León, Facultad de Ciencias Químicas, Ciudad Universitaria, 66451 Nuevo León, Mexico

[2] Centro de Investigación y de Estudios Avanzados del IPN, Unidad Monterrey, PIIT, C.P, 66600 Apodaca, Nuevo León, Mexico

[3] Department of Chemistry and Biochemistry, The University of Texas at Arlington, Arlington, Texas 76019-0065, USA

[4] Centro de Investigación en Materiales Avanzados, S.C., Alianza Norte 202, PIIT, Carretera Monterrey-Aeropuerto Km. 10, C. P, 66628 Apodaca, Nuevo León, Mexico

**Correspondence**
Víctor M. Jiménez-Pérez, Universidad Autónoma de Nuevo León, Facultad de Ciencias Químicas, Ciudad Universitaria, 66451 Nuevo León, Mexico.
Email: victor.jimenezpr@uanl.edu.mx

The fluorescence imaging technologies are becoming the most powerful and noninvasive diagnostic tools in cellular biology and modern medicine where abnormal cell arrangements are associated with diseases. Thus, these techniques require new fluorescent dyes with excellent chemical, physical, and photophysical properties. A series of four new Boron Schiff bases (1–4) has been prepared by condensation between phenylboronic acid with the corresponding ligand. The compounds were characterized by NMR ($^1$H, $^{13}$C, and $^{11}$B), UV/vis, fluorescence spectroscopy, and high-resolution mass spectrometry. The crystal structures of three compounds showed tetracoordinated Boron atoms with semiplanar skeleton ligands. Interesting organoboron response to viscosity on their fluorescence (Φ: more than 3-fold). Additionally, compounds 1 and 2 were found to serve as a fluorescent dye for cell imaging (B16F10, CaCo, and A-431 cells) since it has the capability to rapidly accumulate within the cells and gave bright green fluorescence, it showed low cytotoxicity activity and high photostability in solution. Additionally, the compounds have also been investigated using DFT.

**KEYWORDS**
bioimaging, BOSCHIBAs, high photostability, low cytotoxicity

## 1 | INTRODUCTION

In the recent decade, fluorescent organoboron compounds have gained tremendous attention due to different and interesting applications such as optoelectronic devices,[1] sensors,[2,3] security inks,[4,5] and fluorescent bioimaging (FBI).[6,7] The cellular biology and biomedicine are quite interesting about the advances in fluorescence imaging technologies to identify organelle and cellular abnormalities which are associated with severe diseases and disabilities.[8] It is important to know the anatomy and physiology in the cellular structure and organelles (e.g., mitochondria, the endoplasmic reticulum, lysosomes, Golgi apparatus, and vacuoles). In particular, the cytoplasm is the solution where are suspended some major the organelles and provides mechanical support to

the internal cell structures. Important activities into the cell occur in the cytoplasm such as glycolysis, the breakdown of waste, and cell division. Based on the above mentioned, it is important to design and synthesize new fluorescent cytoplasm markers with suitable photophysical properties and photostability, low cytotoxicity, solubility in polar solvents to be used in the modern cell biology *in vitro* and *in vivo*.[9] Nowadays, the Boron dipyrromethanes (BODIPYs) are the most widely fluorescence organic compounds studied due to the vast range of biochemical and medical applications[10,11] and probably in the second place the Boron diketonates (BODIKEs) where both show selective cytoplasm staining *in vitro* (Figure 1a).[12] However, in the last decade, the Boron Schiff bases (BOSCHIBAs,

Figure 1a) have gained attention due to easy[13] and green synthesis, non-linear optical[14] and linear optical properties,[15] sensitive for solar cells.[16] However, the fluorescent Boron derivatives from Schiff bases are sparse in fluorescent probes (*vide infra*).[17] The biomarkers should show the following characteristics: able to enter cells, good solubility, biocompatibility, chemo-, and photo-stability, high brightness when internalized into cells and minimal cytotoxicity.[18–20] However, at subcellular level most of the diseases are correlated to irregular levels of cellular pH,[21,22] viscosity,[23,24] and oxygen concentration.[25,26]

Because of this, in new researches have been developed biomarkers that respond to one stimulus such as pH, viscosity, oxygen, temperature, and solvent polarity
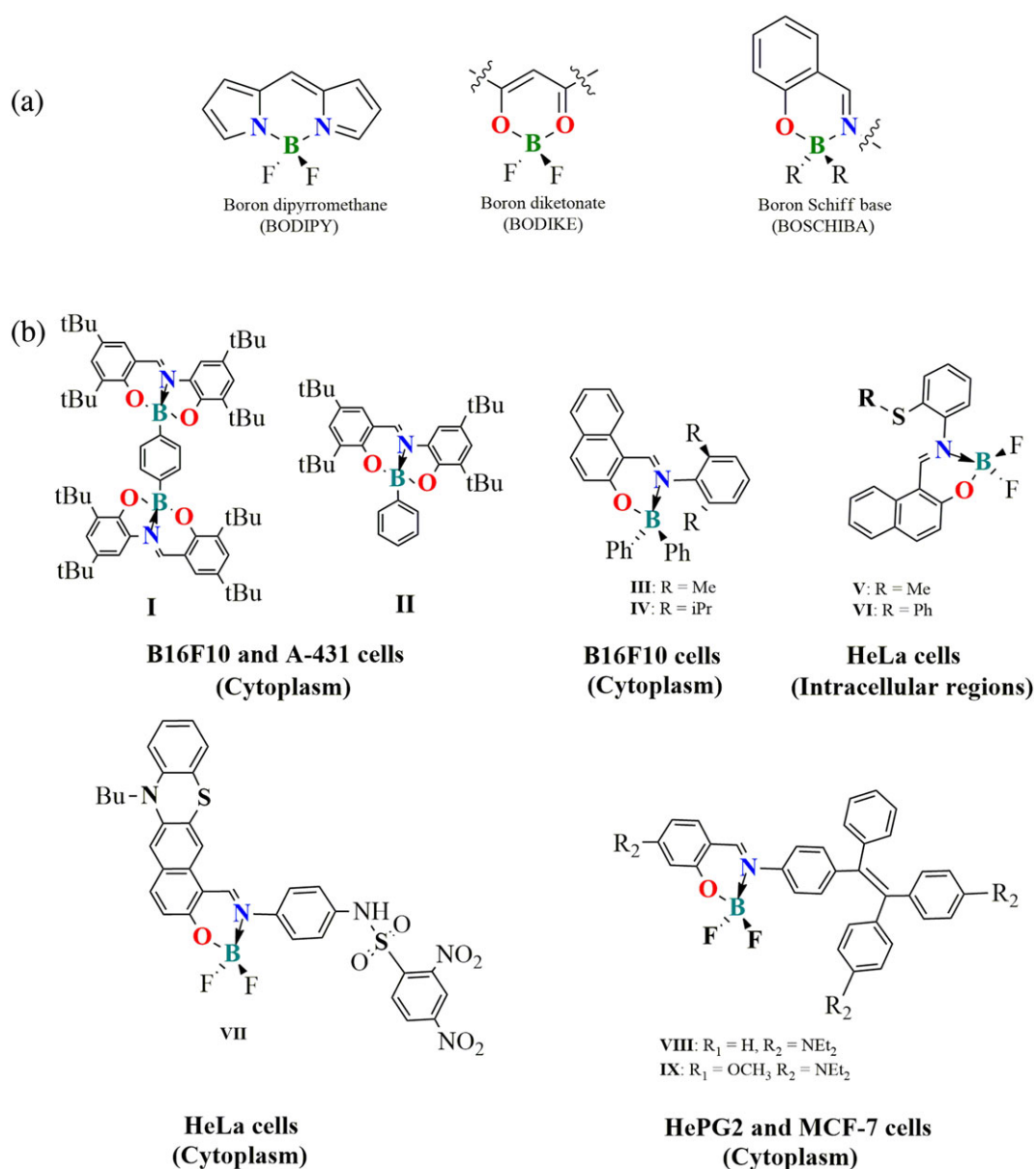


**FIGURE 1** a) Boron derivatives. b) Boron Schiff base compounds as cell staining fluorescent probe *in vitro* (**I-IX**)

with the purpose of developing methods to monitor these parameters at the cellular level.[27] As an example, a BODIPY based molecular sensor reported by Young-Tae Chang, has been used to monitoring in real time the viscosity changes by fluorescence lifetime imaging microscopy (FLIM).[28] Fluorescent dyes to bioimaging must cover important features such as good photophysical, physical, and chemical properties such as high photostability. Recently, Boron Schiff bases BOSCHIBAs have been used to stain cells (Figure 1b).[29]

We have reported and proposed the BOSCHIBAs (I-IV) as a new fluorescent material to staining the cytoplasm *in vitro*. Our synthetic approach is simple and Boron compounds were obtained in moderate yields. The BOSCHIBAs (I and II) exhibit low cytotoxicity level and poor fluorescence staining in B16F10 and A-431 cells treated with 10 μg/ml, also they have low quantum yields (>1%). However, the compound (I) shows the molecular rotor property with the ability to increase the luminescence in a viscous medium.[30] BOSCHIBAs (II-IV) were designed for the same purpose where the compounds showed high stability in aqueous solution and UV radiation, with low cytotoxicity and cytoplasmic staining dyes in B16F10 cells (from 0.1 to 2.5 mg/mL).[17] In order to contribute in the fluorescent imaging technologies, we have been interested in the design and synthesis of Boron Schiff bases as fluorescent dyes for bioimaging. Here, we report the synthesis, characterization, and photophysical properties of BOSCHIBA 2; which show the fluorescence emission change with the increase of media viscosity. The studies were complemented with the cytotoxic activity, cell-imaging experiments; the compounds 1 and 2 have good properties in solution, to be applied as potential cellular biomarkers and biological system.

## 2 | EXPERIMENTAL

## 2.1 | Material and equipment

All starting materials were purchased from Aldrich Chemical Company. Solvents were used without further purification. The ligands L1-L4 were prepared accorded to the method reported[31] as well as compound 1.[17] Melting points were performed on an Electrothermal Mel-Temp apparatus and are uncorrected. High- resolution mass spectrum was obtained by LC/MSD-TOF on an Agilent Technologies instrument with APCI as ionization source. Infrared spectra were recorded using a Bruker Tensor 27 FT-IR spectrophotometer equipped with a Pike Miracle™ ATR accessory with a single reflection ZnSe ATR crystal. UV spectra were obtained with a Perkin Elmer Lambda 356 U*V*/Vis spectrophotometer

and emission measurements were performed on a Fluorolog-3 Spectrofluorometer. $^1$H, $^{13}$C and $^{11}$B NMR spectra were recorded on a Bruker advance DPX 400. Chemical shifts (ppm) are relative to $(CH_3)_4Si$ for $^1$H and $^{13}$C. $^{11}$B NMR spectra were referenced externally to $Et_2O \cdot BF_3$. Mass spectra were recorded on an AB Sciex API 2000 LC/MS/MS System.

## 2.2 | Crystal structure determination

The X-ray intensity data of crystals of 1 and 2 were measured at 100(2) K on a Bruker D8 Quest with a Photon 100 CMOS detector equipped with an Oxford Cryosystems 700 series cooler, a Triumph monochromator, and a Mo Kα fine-focus sealed tube (λ = 0.71073 Å). X-ray intensity data of crystals of 3 were measured at 100(2) K on a SMART APEX II CCD area detector system equipped with an Oxford Cryosystems 700 series cooler, a graphite monochromator, and a Mo Kα fine-focus sealed tube (λ = 0.71073 Å). Intensity data were processed using the Bruker Apex program suite. Absorption corrections were applied by using SADABS.[32] Initial atomic positions were located by direct methods using XS or SHELXT,[33] and the structures of the compounds were refined by the least-squares method using SHELXL[34] within Olex2[35] GUI. All the non-hydrogen atoms were refined anisotropically. The hydrogen atoms were placed in geometrically idealized positions and constrained to ride on their parent atoms with relative isotropic displacement parameters. The CCDC for 1 (1533019), 2 (1533020) and 3 (1533018) contain the supplementary crystallographic data. These data can be obtained free of charge via http://www.ccdc.cam.ac.uk/conts/retrieving.html or from the Cambridge Crystallographic Data Centre (CCDC), 12 Union Road, Cambridge, CB2 1EZ, UK).

## 2.3 | General procedure of synthesis of 1–4

### 2.3.1 | 4,6-diphenylnaphtho[1,2-h] [1,3,5,6,2] dioxadiazaboronine (1)

A solution of L1 [(E)-N′-((2-hydroxynaphthalen-1-yl) methylene)benzohydrazide)] (0.29 g, 1 mmol) and phenylboronic acid (0.122 g, 1 mmol) in acetonitrile was heated under reflux for 48 hrs. The reaction mixture was slowly cooled to room temperature, the solvent is evaporated and adding ethyl acetate, it was allowed to evaporate slowly at 10 days, yellow crystals is obtained. The compound is soluble in chloroform. Yield of 0.28 g (74%). M. P.: 152 °C. $^1$H NMR (400 MHz, DMSO-$d_6$, 298 K) δ = 7.09 (m, 1H, H3), 7.33 (m, 1H, H15), 7.39 (m, 1H, H7), 7.43 (m, 1H, H-*m*), 7.45 (m, 2H, H-*o* and H-*p*), 7.52 (t, 1H, H14), 7.57 (m, 1H, H8), 7.67 (m, 1H, H16), 7.87

(m, 2H, H4 and H6), 8.11 (d, 1H, H9), 8.71 (s, 1H, H11). $^{13}$C NMR (100 MHz, DMSO-$d_6$, 298 K) δ = 110.43 (C1), 119.79 (Cp), 121.03 (C4), 123.74 (C7), 127.16 (C5), 127.68 (C15), 128.32 (C3), 128.42 (C10), 128.76 (C14), 128.97 (C8), 129.27 (C6), 131.45 (Cm), 131.53 (C13), 132.12 (C16), 137.47 (C9), 141.53 (C11), 155.61 (C2), 170.89 (C12). HETCOR [$\delta_H/\delta_C$]: 7.20/7.80 (H3/C3), 7.21/127.68 (H15/C15), 7.41/124.91 (H7/C7), 7.43/131.45 (H-$m$/C-$m$), 7.45/120.64 (H-$p$/C-$p$), 7.52/128.76 (H14/C14), 7.57/128.97 (H8/C8), 7.59/132.98 (H16/C16), 7.8/129.27 (H6/C6), 7.84/121.03 (H4/C4), 8.03/138.33 (H9/C9), 8.85/142.11 (H11/C11). COSY [$\delta_H/\delta_H$]: 7.20/7.84 (H3/H4), 7.80/7.41 (H6/H7), 7.57/8.03 (H8/H9), 7.52/7.21 (H14/H15), 7.21/7.59 (H15/H16). $^{11}$B NMR (128 MHz, CDCl$_3$, 298 K) δ = 8.06 ppm. TOF MS: Calcd. for [C$_{24}$H$_{17}$N$_2$O$_2$B + H]$^+$: 377.1467; Found: 377.1462 (error 0.1251 ppm). UV–Vis (CHCl$_3$): $\lambda_{abs/max}$ 426 nm.

## 2.3.2 | 4-(6-phenylnaphtho[1,2-h][1,3,5,6,2] dioxadiazaboronin-4-yl) phenol (2)

A solution of **L2** [(E)-4-hydroxy-N′-((2-hydroxynaphthalen-1-yl)methylene)benzohydrazide] (0.34 g, 1.1 mmol) and phenylboronic acid (0.15 g, 1.3 mmol) in acetonitrile was heated under reflux for 48 hrs. The reaction mixture was slowly cooled to room temperature, the solvent is evaporated and adding THF at −10 °C, in 24 hours to give yellow crystals. The compound is soluble in chloroform and THF. Yield of 0.35 g (81%). M. P.: 170 °C. $^1$H NMR (400 MHz, THF-$d_8$, 298 K) δ = 6.93 (d, 2H, H15 and 17), 7.10 (t, 1H, H-$m$), 7.35 (m, 3H, H-$o$, $p$, and H3), 7.46 (t, 1H, H8), 7.7 (d, 2H, H14 and H18), 7.99 (m, 2H, H4 and H7), 8.11 (d, 2H, H6 and H9), 9.10 (s, 1H, H11), 9.29 (s, 1H, OH). $^{13}$C NMR (100 MHz, THF-$d_8$, 298 K) δ = 116.50 (C15 and C17), 121.29 (C-$p$), 122.37 (C7), 125.37 (C-$o$), 129.78 (C14 y C18), 131.60 (C6), 132.14 (C3), 138.31 (C4), 143.62 (C11), 157.44 (C2), 163.22 (C12), 172.61 (C16). HETCOR [$\delta_H/\delta_C$]: 6.95/116.54 (H15 and 17/C15 and 17), 7.30/125.38 (H-$o$/C-$o$), 7.37/121.21 (H-$p$/C-$p$), 7.40/132.15 (H3/C3), 7.45/129.38 (H8/C8), 7.72/129.78 (H14 and 18/C14 and 15), 7.96/138.36 (H4/C4), 7.96/122.31 (H7/C7), 8.16/131.6 (H6 and 9/C6 and 9), 9.08/143.57 (H11/C11). $^{11}$B NMR (128 MHz, THF-$d_8$, 298 K) δ = 7.32 ppm. TOF MS: Calcd. for [C$_{24}$H$_{17}$N$_2$O$_3$B + H]$^+$: 393.1405; Found: 393.1403 (error 0.5300 ppm). IR ν (cm$^{-1}$) 2945 (C-H$_{aromatic}$), 1603 (C=N). UV–Vis (CHCl$_3$): $\lambda_{abs/max}$ 423 nm.

## 2.3.3 | (E)-(2-hydroxy-1-naphthalidene)4-nitro-benzohydrazidato-phenyl-boron (3)

A solution of **L3** [(E)-(2-hydroxy-1-naphthalidene)-4-nitrobenzohydrazide] (0.335 g, 1 mmol) and phenylboronic

acid (0.122 g, 1.0 mmol) in acetonitrile was heated under reflux for 48 hours. The reaction mixture was slowly cooled to room temperature, the solvent is evaporated and adding THF at −10 °C, in 24 hours to give orange crystals. The compound is soluble in chloroform and THF. Yield of 0.38 g (90%). M. P.: 326 °C. $^1$H NMR (400 MHz, CDCl$_3$) δ: 7.20 (m, 2H, H-m), 7.22 (m, 1H, H-p), 7.39 (m, 1H, H-o), 7.43 (d, 1H, H-3), 7.47 (st, 1H, H-7), 7.62 (t, 1H, H-8), 7.83 (d, 1H, H-6), 7.89 (d, 1H, H-4), 8.08 (d, 1H, H-9), 8.34 (d, 2H, H-15,17), 8.38 (d, 2H, H-14,18), 8.92 (s, 1H,H-11) ppm. $^{13}$C NMR (100 MHz, CDCl$_3$) δ: 112.12 (C-1), 120.61 (C-3), 121.13 (C-4), 123.94 (C-15,17), 125.29 (C-7), 127.81 (C-m), 128.55 (C-5), 128.60 (C-p), 129.37 (C-8), 129.49 (C-6), 129.67 (C-14,18), 131.34 (C-o), 131.40 (C-i), 131.59 (C-10), 133.34 (C-13), 139.37 (C-9), 144.27 (C-11), 150.41 (C-16), 157.20 (C-2), 169.55 (C-12) ppm. HETCOR [$\delta_H/\delta_C$]: 7.20/127.81 (H-m/C-m), 7.22/128.60 (H-p/C-p), 7.39/131.34 (H-o/C-o), 7.43/120.61 (H-3/C-3), 7.47/125.29 (H-7/C-7), 7.62/129.37 (H-8/C-8), 7.83/129.49 (H-6/C-6), 7.89/121.13 (H-4/C-4), 8.08/139.37 (H-9/C-9), 8.34/123.94 (H-15,17/C-15,17), 8.38/129.67 (H-14,18/C-14,18), 8.92/144.27 (H-11/C-11) ppm. COSY [$\delta_H/\delta_H$]: 7.43/7.89 (H-3/H-4), 7.83/7.47 (H-6/H-7), 7.62/8.08 (H-8/H-9), 8.38/8.34 (H-14,18/H-15,17) ppm. Anal. Calc. for C$_{24}$H$_{16}$BN$_3$O$_4$: C; 68.43. H; 3.83. N; 9.98, Found: C; 68.70. H; 3.94. N; 7.73. TOF MS: Calcd. for [C$_{24}$H$_{16}$N$_3$O$_4$B + H]$^+$: 422.1200; Found: 422.1307 (Error = 1.50 ppm). IR$_{vmax}$ (ATR): 3082, 1634 (C=O), 1531, 1453, 1338, 1191, 1089, 907, 863, 737, 701 cm$^{-1}$. UV/Vis (CHCl$_3$): $\lambda_{abs/max}$: 374 nm.

## 2.3.4 | 9,11-di-tert-butyl-2,4-diphenylbenzo [h] [1,3,5,6,2] dioxadiazaboronine (4)

A solution of **L4** [(E)-N′-(3,5-di-tert-butyl-2-hydroxybenzylidene)benzohydrazide] (0.35 g, 1 mmol) and phenylboronic acid (0.15 g, 1.3 mmol) in acetonitrile was heated under reflux for 48 hrs. The reaction mixture was slowly cooled to room temperature; precipitated solid is filtered and washed with hexane. The compound is partially soluble in DMSO and THF. Yield of 0.361 g (82%). M. P.: 158–160 °C. TOF MS: Calcd. for [C$_{28}$H$_{31}$N$_2$O$_2$B $^+$H]$^+$: 439.2551, Found: 439.2552 (error 0.0471 ppm).

## 2.3.5 | Absorbance, emission and luminescence quantum yields

UV–Vis absorption spectra were measured on a Perkin Elmer Lambda 365 spectrophotometer. Optical band gap (Eg) was determined from the intercept with the X axis of the tangent of the absorption spectrum drawn at absorbance of 0.1. The emission spectra have been recorded with a Fluorolog-3 Spectrofluorometer, by exciting

10 nm below the longer wavelength absorption band. Fluorescence quantum yields in solution were determined according to the procedure reported in the literature[36] by using quinine sulphate in $H_2SO_4$ 0.1 M as the standard. Three solutions with absorbance at the excitation wavelength lower than 0.1 were analyzed for each sample and the quantum yield was averaged. The viscosity of the solvent mixture (methanol/glycerol) was determined in ViscoLab 3000 Cambridge.

### 2.3.6 | Cytotoxicity assays in cells and bioimaging

Cytotoxic effects of compounds **1** and **2** were analyzed on murine melanoma cells, B16F10 (ATCC, CRL-6475. Manassas, VA). Cells were maintained in 25 cm² flasks using Gibco Advanced DMEM/F12 medium (Fisher Scientific, Pittsburgh, PA), at 37 °C in a 5% $CO_2$ and 95% air controlled atmosphere. For cytotoxicity assays cells were seeded in 96 wells plates at a cells density of $5 \times 10^3$ cells per well in 100 μl of medium and let rest for 24 hours. The compounds were added at concentration of 0.1, 1, 2.5, 5, and 10 μg/ml and cells treated with dimethyl sulfoxide (DMSO Sigma-Aldrich Co, St. Louis, MO, USA) were used as controls. Forty-eight hours later cells viability was determined by adding 10% alamar Blue. Color change was recorded in an ELISA Microplate Reader (Biotek Multiskan ELX800, BioTek Instruments, Inc., Winooski, VT, USA) at dual wavelength of 570 and 600 nm following manufacturer's instructions. In order to analyze the bioimaging capabilities of **1** and **2** in B16F10, CaCo (human epithelial colorectal) and A431 (human epidermoid) cells were seeded on sterile coverslips in 12 wells plates at a cell density of $5 \times 10^4$ cells per well in 2 ml of medium. 24 hours later cells were exposed for 2 hr to the organoboron compounds at a concentration of 10 μg/ml, washed twice with 1X PBS, mounted on microscope glass slides using Vectashield (Vector Laboratories, Inc. Burlingame, CA, USA) and analyzed by confocal microscopy in a Leica TCS SP5 Confocal System. Samples were excited at 405 nm and its blue fluorescence emission recorded at 420–550 nm, or excited at 488 nm and green fluorescence emission recorded at 500–600 nm.

### 2.3.7 | Computational details

All calculations were performed using GAUSSIAN 09 software package.[37] The geometries of **1–4** were fully optimized with the B3LYP 1/6-31G(d,p) method.[38] The minima were characterized by calculating their vibrational modes at the same level of theory. Results were visualized using the Chemcraft program v1.7.

## 3 | RESULTS AND DISCUSSION

### 3.1 | Synthesis and solution characterization

The compounds **1–4** were obtained in moderate yields (74–90%) by second step of condensation between phenylboronic acid with the corresponding ligand under reflux in acetonitrile (Scheme 1). The resulting BOSCHIBAs were soluble in several organic solvents while that **4** was unstable in solution at room temperature (25 °C) after one week where the UV–Vis spectrum showed the formation of the corresponding ligand. The compounds were fully characterized by NMR (¹H, ¹¹B, and ¹³C), and mass spectrometry. High-resolution mass spectra of compounds **1**, **2** and **4** show the base peak which corresponds to the molecular ion peak (**1**: 377.1462, **2**: 393.1403, **4**: 439.2555), the molecules show a fragment due to the loss of ring of benzene bonded to Boron atom, obtaining the fragment of the ligand (L1-L2 and L4).

Interesting to mention for compound **1** and **2**, the formation of a dimer is observed, possibly due to the intermolecular interactions of the aromatics (Scheme S1). The compounds **1–3** were characterized by single crystal X-ray diffraction. Likewise, the existence of the N → B coordination bond was evidenced by ¹¹B NMR spectra for the compounds **1** and **2**, with one broad signal at 8.06 and 7.32 ppm respectively (see Table S1), which is in agreement with the existence of tetra-coordinated Boron atom.[39]

### 3.2 | X-ray structures

Suitable single crystals of **1–3** were obtained by slow evaporation of ethyl acetate and tetrahydrofuran mixture.
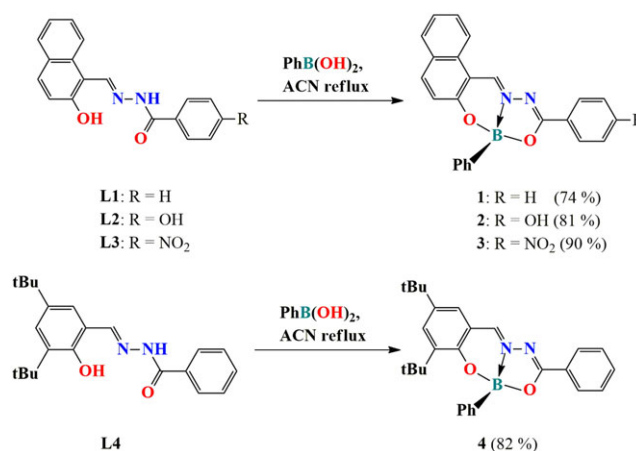


**SCHEME 1**  Synthesis of Boron compounds **1–4**

X-ray analyses, their molecular structures, bond lengths, and angles are shown in Figure 2. X-ray crystallographic parameters are summarized in Tables S2 and S3. The compounds **1** and **3** crystallized in the triclinic P-1 while **2** in the monoclinic P2$_1$/n space groups. There are two chemically similar but crystallographically different molecules of **2** and four THF molecules in the asymmetric unit. Both **1** and **2** formed yellow square blocks whereas **3** produced orange prisms.

The crystal structures of **1–3** show tetracoordinated Boron atoms and the formation of fused five and six-member heterocycles. Boron atoms adopt distorted tetrahedral geometry. The B-O bond lengths **1** [1.468(2) - 1.500(2) Å], **2** [1.469(2) - 1.499(2) Å] and **3** [1.467(2) - 1.503(2) Å] are characteristic for tetra-coordinated Boron complexes, and agree well with reported molecules.[39a] The B-N bond lengths **1** [1.564(1) Å], **2** [1.562(2) Å] **3** [1.565(2) Å] indicate a strong interaction of the nitrogen atom with Boron atom, which is confirmed by the tetrahedral character of **1**: 88.58, **2**: 88.66 and **3**: 89.16% for each molecule.[40] The Boron atom resides outside the ligand plane. The crystal structures of **1–3** also show intermolecular interactions such as π-π (the shortest C---C distances) in the range from 3.339 Å to 3.378 Å, the compound **2** shown intermolecular interactions H-bonding between O-H and oxygen of THF, and other molecule of same compound [C(17)-H(17)---B(2), 3.056 (2)], [C(41)-H(41)---B(1), 3.141 (2)], [C(41)-H(41)---O(1), 2.600 (1)], [C(18)---H(56B), 2.892 (1)], [C(12)---H(54A), 2.889 (1)], [C(1)-H(1)---O(9), 2.293 (1)] Å see Figure S17. Compounds **4** was unstable in the solution state.

## 3.3 | Photophysical characterization

The optical properties for compounds were obtained in spectroscopic grade tetrahydrofuran (Table 1). Figure 3a shows the electronic absorption spectra of the compounds **1–3**, it shows the main absorption band in a range from 319 to 346 nm attributed to the π-π* electronic transition of the molecules. The molar extinction coefficients (ε) of **1–3** were in the range of 13000–133000 M$^{-1}$ cm$^{-1}$ The fluorescence spectra of **1–3** in Figure 3b. The compounds **1** and **2** show broad blue emission bands at 488, and 479 nm (See Table 1) in the case of **3** its substitution with a withdrawing group (-NO$_2$) shifted to the violet region. The fluorescence quantum yield (Φ$_F$) is very weak for all molecules.

## 3.4 | Viscosity studies

Monitoring of intracellular viscosity would be important to understand the pathological effects associated with abnormal viscosity levels in living systems[41]; Due to the instability of **3** and the low solubility of **1** in the methanol/glycerol mixture, the effect of the viscosity was not possible to carry out. The viscosity analysis revealed that compound **2** present a viscosity-dependent behavior. (Figure 4, Table S4).[42] We utilized the Fröster–Hoffmann equation to correlate the relationship between the emission intensity of compound **2** and the solvent viscosity[43]; it has a moderate slope but higher correlation which confirms the best linear relationship between log η and log Φ$_F$ (R$^2$ = 0.82) (see Figure S18).
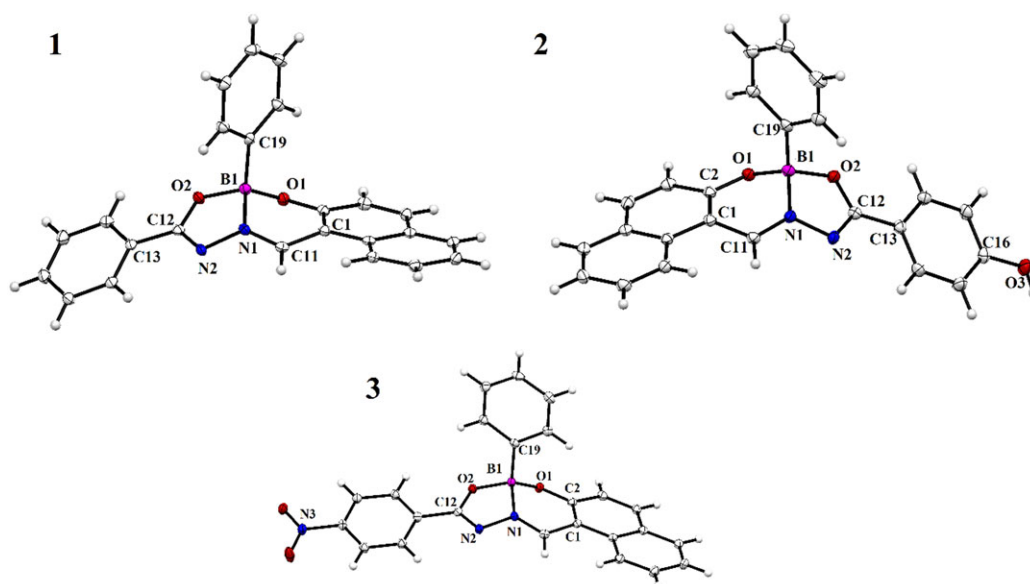


**FIGURE 2** View of the structure of **1–3**. Ellipsoids are drawn at the 30% probability level

**TABLE 1** Photophysical properties of **1–3** in THF

| Comp | $\lambda_{abs}$ [nm] | $\varepsilon*10^4$ [M$^{-1}$cm$^{-1}$] | Eg [eV] | $\lambda_{em}$ [nm] | $\Delta\nu$ [cm$^{-1}$] | $\Phi_F$ [%] |
|---|---|---|---|---|---|---|
| **1** | 342(423) | 1.90(1.80) | 2.63 | 488 | 3232 | 0.2 |
| **2** | 346(424) | 13.30(7.20) | 2.63 | 479 | 2621 | 0.8 |
| **3** | 323(374) | 3.80(5.50) | 2.94 | 430 | 3428 | 0.4 |

$\lambda_{abs}$: two bands of absorption (maximum), $\varepsilon$: molar extinction coefficients for two absorption, Eg: optical band gaps, $\lambda_{em}$: emission maximum, $\Delta\nu$: Stoke's shift, $\Phi_F$: fluorescence quantum yield.

The initial fluorescence intensity of compound **2** in methanol is higher than the fluorescence intensity in THF, which indicates the possible polarization of the compound in polar solvents. However, in glycerol solvent, the fluorescence intensity of compound **2** increased by 3.0 fold. This viscous medium generates the restriction to rotation of phenyl rings (Figure S19) and the compound act as molecular rotors with viscosity fluorescence sensitivity. The compound **2** exhibits sensitivity towards the viscosity of the environment. Further, we studied the effect of pH on the fluorescence behavior of compounds.

## 3.5 | Cytotoxicity assays in cells and bioimaging

Potential applications of these BOSCHIBAs include cell imaging and, as stated above, one the characteristics, besides staining, that would make a biomarker more attractive it would be its low cytotoxicity. B16F10 melanoma cells were treated with different concentrations of compounds **1** and **2**. Both compounds showed to be innocuous to cells at the lower tested concentration (0.1 μg/ml). Compound **1** was slightly toxic when tested at higher concentrations; however, its cell viability never was less than 70% (Figure S25, blue line). Compound **2** showed a similar behavior except that at the higher
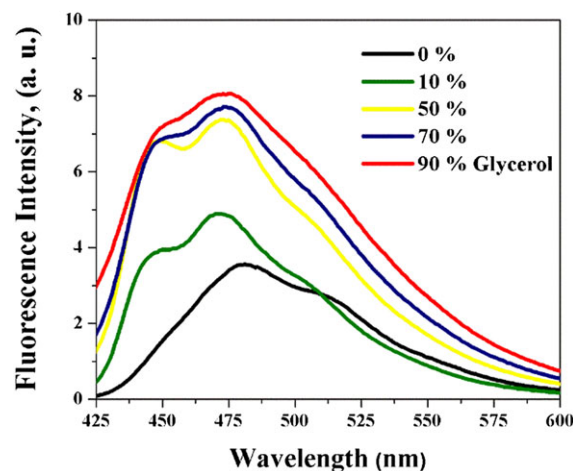


**FIGURE 4** Fluorescence spectra of compound **2** in binary mixtures of methanol and glycerol in different ratios

tested concentration (10 μg/ml) resulted more toxic with 80% of viability (Figure S25, red line). Based on previous report by our group, the substitution of tin by Boron showed to be beneficial to cells viability as cytotoxicity dropped significantly.[44] Importantly the **1–2** were shown to exhibit low cytotoxicity and high levels of cell viability (>80%) at 1 μg/ml. However, the (**1–2**) show lower viability values (<70%) at 5 μg/ml compared with similar molecules reported, due to it were placed for an incubation time of 48 hr.[45] This data makes our compounds good prospects for new fluorescent cell marker when cells viability is important to maintain intact. The capacity of **1** and **2** to produce fluorescence staining in cells was determined on B16F10 cells. When fluorescence was excited at 405 nm, the compounds emitted blue fluorescence. However, **2** showed a stronger cytoplasm mainly stain (Figure 5, E and H). Excitation at 488 nm resulted in a green fluorescence stain by compounds **1** and **2** (Figure 5, F and I). These results show that complexes can readily penetrate cell membranes and distribute through the cytoplasm without apparent degradation, as their fluorescence remained intact.
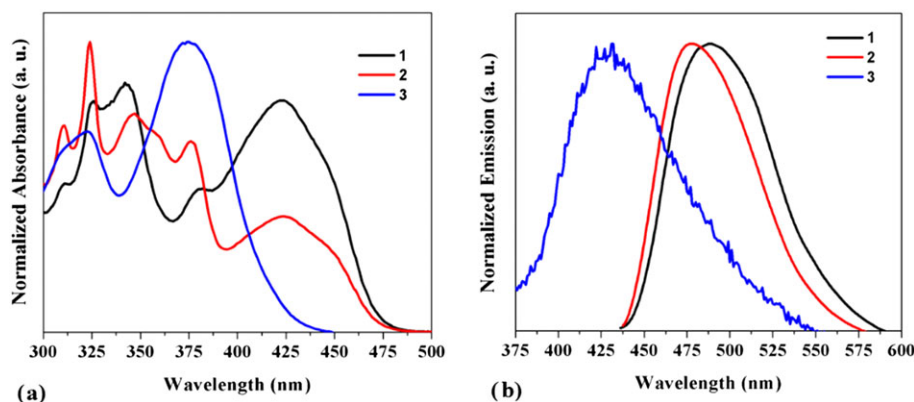


**FIGURE 3** a) Absorption spectra of **1–3**. b) Emission spectra of **1–3** in THF

Although fluorescence is observed along the whole cell, there is a higher emission at certain subcellular compartments that resemble localization of the endoplasmic reticulum (Figure 6). CaCo and A-431 cells were used to compare the staining capacity of **1** and **2** in other cells. They were incubated at the concentration of 10 μM for 2 hr with CaCo and A-431 cells at 37 °C. Both compounds were found to rapidly accumulate within the cells and gave bright green fluorescence, as shown in Figure 7.

In the Figure 7 B) and F) for compound **1** the two cell lines are well defined, however, for compound **2**, Figure 7 D) and H), agglomeration of cells is observed. The bioimaging show good permeability of the compounds, retaining in the cells, similar behavior with the HeLa cells. Overall, compound **2** showed to be the best fluorescent marker in this study. This might be the result from the –OH substituent group present in the molecule,

which confers a greater solubility in polar solvents that translate in a better bio distribution inside the cells.

## 3.6 | Photo-stability testing and stability in aqueous DMSO solutions

For bioimaging applications, it is desirable the fluorescent dye *in vitro* not show any photophysical change under the confocal laser. The photostability studies of **1** and **2** are given in the electronic supplementary information. Figure S20 shows the compounds degradation under UV light irradiation at 365 nm by time intervals from 10 to 40 min, and monitored by UV–vis spectroscopy. Photostability studies revealed the compounds **1** and **2** show a higher resistance to degradation (~7% at 20 min). In the case of **2** after being irradiated from 30 to 40 minutes, compound **1** displays a marked hysteresis
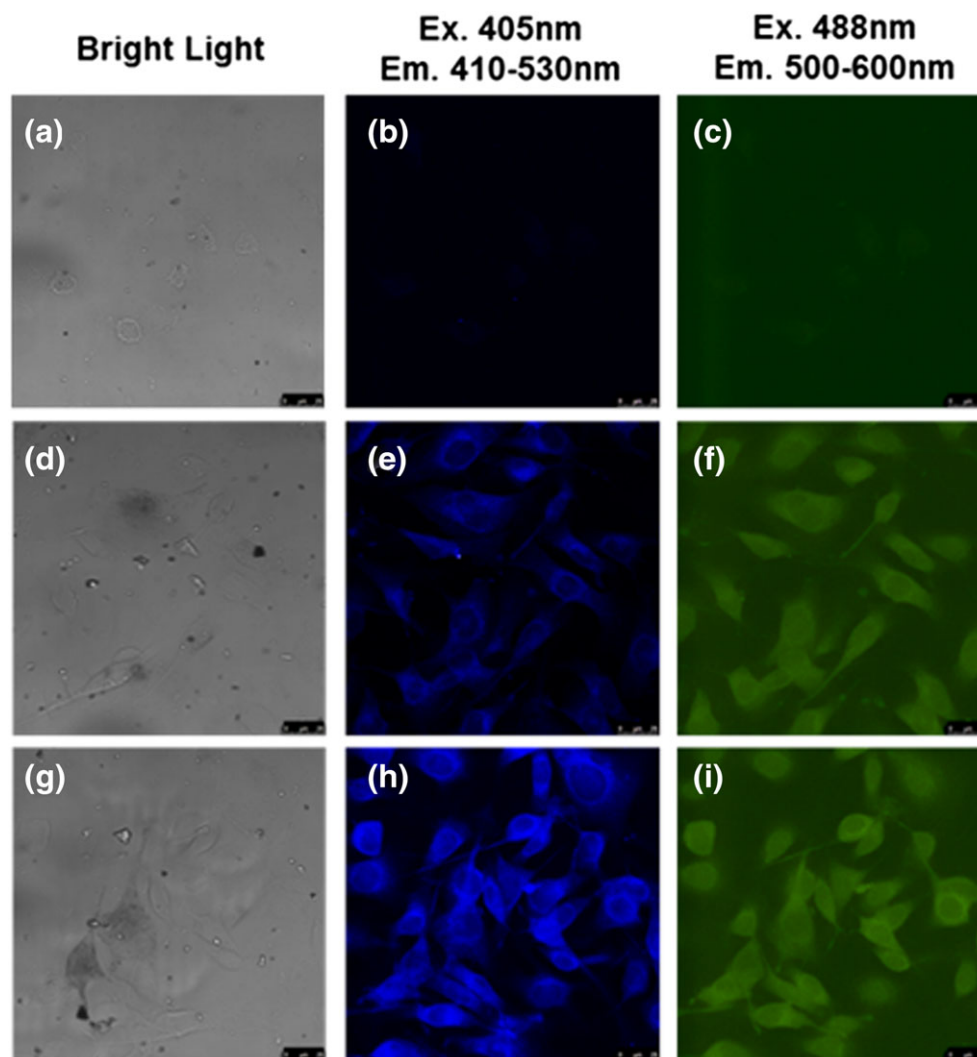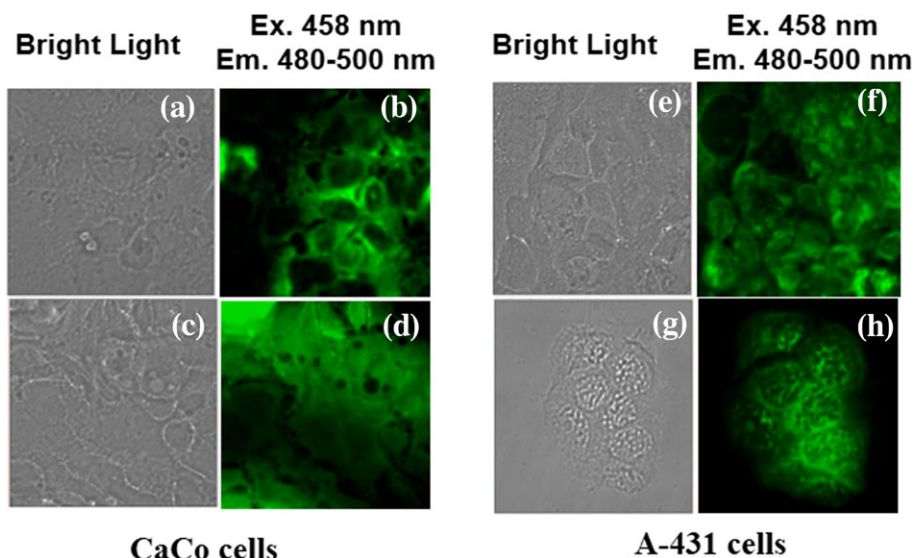


**FIGURE 5** Bioimaging with compounds **1** and **2**. B16F10 cells were treated 2 hr with each complex and analyzed by confocal microscopy. Panels A-C, DMSO treated cells; panels D-F, complex **1**; panels G-I, complex **2**. Scale bars represent 25 μm
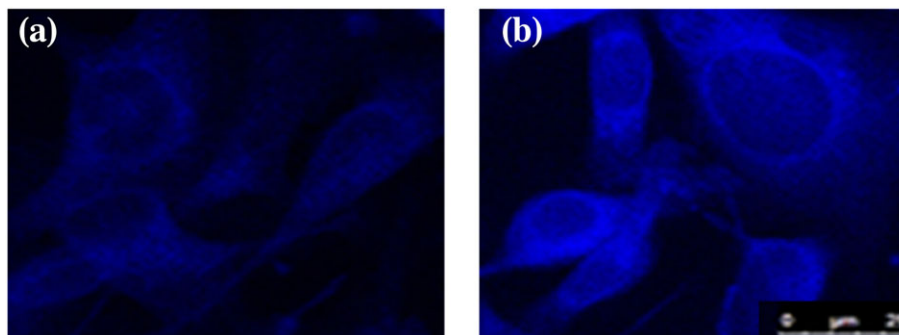
**FIGURE 6** Bioimaging with compounds **1** (A) and **2** (B). B16F10 cells were treated 2 hr with each complex and analyzed by confocal microscopy. Scale bars represent 25 μm



**FIGURE 7** Bioimaging with compounds **1** and **2**. Cells were treated 2 h with each complex and analyzed by confocal microscopy. CaCo cells, Panels A-B, **1**; panels C-D, **2**. A-431 cells, Panels E-F, **1**; panels G-H, **2**

in their absorbance against irradiation curve with respect the assays performed in a range from 10 to 20 min. The effect of this hysteresis might be ascribed to the monomer decomposition toward the free-ligand as shows both UV–Vis spectra (Figure S22, S24). Likewise, the stability in aqueous solutions at 1% *v/v* of DMSO for compounds were evaluated under the same experimental condition without photoirradiation (Figure S21). The analysis demonstrated that **1** and **2** to be highly stable in aqueous DMSO solution even after 60 min because there were not any important changes in the absorption peaks (See figure S22).

## 3.7 | DFT calculations

The compound geometries of **1–4** were optimized by using the B3LYP 6-31G(d,p) method. In Table S3, we

can see experimental and calculated values of selected angles and bond lengths. As we can see in Table S3, the calculated values are in good agreement with those obtained from the X-ray structure. Figure 8 show plots of the highest occupied molecular orbitals (HOMO) and lowest unoccupied molecular orbitals (LUMO) of boronates, HOMO surfaces for **1–3** display electron density localized on the naphthyl group. Significantly the energy value that restricts the free rotation of the aromatic ring, we were manually rotation of the aromatic ring every 30°, for **2**, it showed similar rotation barriers in each conformer. The UV–Vis spectra of **1–4** were calculated at the same level of theory. The calculated absorption bands are located at 374–455 nm (Table S5), which are in agreement with the experimental data (415–465 nm). The absorption bands can be assigned to the $S_0$-$S_1$ transitions, due to the $\pi \rightarrow \pi^*$ electronic transitions through the molecule.
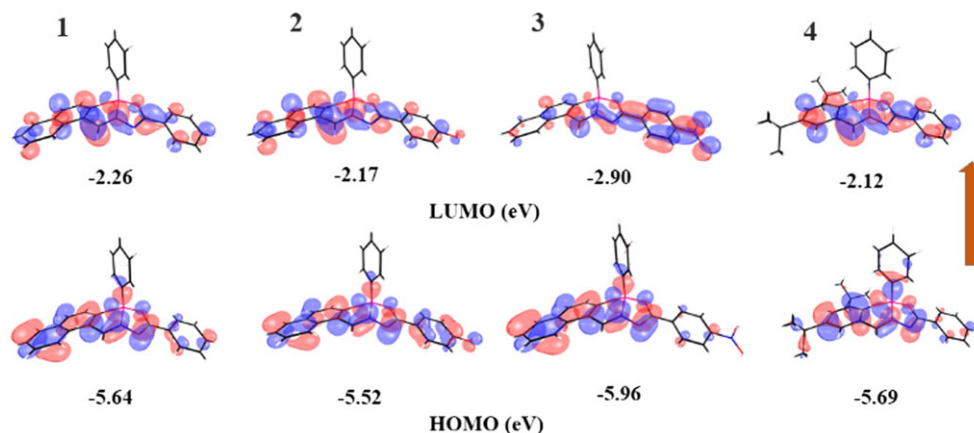
**FIGURE 8** HOMO and LUMO orbitals, and their energies involved in the electronic transitions for **1–4**

## 4 | CONCLUSIONS

In summary, we describe the synthesis, spectroscopic characterization, and fluorescent behavior of a series of new compounds derived from Schiff bases. Interestingly, **1** and **2** have shown low cytotoxicity and very cell-membrane-permeable (B16F10, CaCo, and A-431 cells), which allowed them to diffuse into the cells and be retained within them. Additional both compounds show high stability in aqueous DMSO solution. These properties demonstrate that these molecules can act as good for potential medical application and capacity of staining cells. From the synthetic and design of this BOSCHIBAs chemistry viewpoint, chemical modification in both sides of Schiff base ligands, it would offer a plethora of derivatives in the near future with better physical, chemical, and photophysical properties. The fluorescence intensity increased to compound **2** when was in a viscosity media; thanks to this features, compound **2** is an excellent candidate to be used to distinguish cancer and normal cells.

## CONFLICT OF INTEREST

There are no conflicts to declare.

## ORCID

*Blanca M. Muñoz-Flores* [iD] https://orcid.org/0000-0003-3307-7242

*H.V. Rasika Dias* [iD] https://orcid.org/0000-0002-2362-1331
*Víctor M. Jiménez-Pérez* [iD] https://orcid.org/0000-0003-4306-2482

## REFERENCES

[1] D. Li, H. Zhang, Y. Wang, *Chem. Soc. Rev.* **2013**, *42*, 8416.

[2] Y. Qi, W. Xu, R. Kang, N. Ding, Y. Wang, G. He, Y. Fang, *Chem. Sci.* **2018**, *9*, 1892.

[3] C. R. Wade, A. E. J. Broomsgrove, S. Aldridge, F. P. Gabbaï, *Chem. Rev.* **2010**, *110*, 3958.

[4] F. Wenyan, Z. Yuyang, Z. Gaobin, K. Lin Kong, Y. Longmei, Y. Jiaxiang, *Cryst. Eng. Comm.* **2017**, *19*, 1294.

[5] L. Gu, R. Liu, H. Shi, Q. Wang, G. Song, X. Zhu, S. Yuan, H. Zhu, *J. Fluoresc.* **2016**, *26*, 407.

[6] S. Krajcovicova, J. Stankova, P. Dzubak, M. Hajduch, M. Soural, M. Urban, *Chem. – Eur. J.* **2018**, *24*, 4957.

[7] L. Yang, Y. Liu, X. Zhou, Y. Wu, C. Ma, W. Liu, C. Zhang, *Dyes Pigm.* **2016**, *126*, 232.

[8] J. Berrones-Reyes, C. C. Vidyasagar, B. M. Muñoz Flores, V. M. Jiménez Pérez, *J. Lumines.* **2018**, *195*, 290.

[9] T. D. Ashton, K. A. Jolliffe, F. M. Pfeffer, *Chem. Soc. Rev.* **2015**, *44*, 4547.

[10] T. Kowada, H. Maeda, K. Kikuchi, *Chem. Soc. Rev.* **2015**, *44*, 4953.

[11] Z. Guo, S. Park, J. Yoon, I. Shin, *Chem. Soc. Rev.* **2014**, *43*, 16.

[12] For BODIPYS. Rabhi, I. Rabhi, B. Trentin, D. Piquemal, B. Regnault, S. Goyard, T. Lang, A. Descoteaux, J. Enninga, L. Guizani-Tabbane, *PLOS ONE* **2016**, *11*, 0148640. For Diketoiminates: K. Tanaka, Y. Chujo, NPG Asia Materials. **2015**, *7*, 223 (1–15), C. Peng-Zhong, N. Li-Ya, C. Yu-Zhe, Y. Qing-Zheng, *Coord. Chem. Rev.* **2017**, *350*, 196.

[13] C. Glotzbach, U. Kauscher, J. Voskuhl, N. S. Kehr, M. C. A. Stuart, R. Fröhlich, H. J. Galla, B. J. Ravoo, K. Nagura, S. Saito, S. Yamaguchi, E.-U. Würthwein, *J. Org. Chem.* **2013**, *78*, 4410.

[14] B. M. Muñoz Flores, R. Santillan, M. Rodríguez, J. M. Méndez, M. Romero, N. Farfán, P. G. Lacroix, K. Nakatani, G. Ramos-Ortíz, J. L. Maldonado, *J. Organomet. Chem.* **2008**, *693*, 1321.

[15] S. Romero-Servin, M. de Anda Villa, R. Carriles, G. Ramos-Ortiz, J.-L. Maldonado, M. Rodríguez, M. Güizado-Rodríguez, *Materials* **2015**, *8*, 4258.

[16] R. Chan-Navarro, V. M. Jiménez-Pérez, B. M. Muñoz-Flores, H. V. Rasika Dias, I. Moggio, E. Arias, G. Ramos-Ortíz, R. Santillán, C. García, M. E. Ochoa, M. Yousufuddin, N. Waksman, *Dyes Pigm.* **2013**, *99*, 1036.

[17] M. M. Corona-López, V. M. Jiménez Pérez, R. Chan-Navarro, M. Ibarra-Rodríguez, H. V. R. Dias, A. Chávez-Reyes, B. M. Muñoz-Flores, *J. Organomet. Chem.* **2017**, *852*, 64.

[18] a) P. J. Campagnola, L. M. Loew, *Nature Biotech.* **2003**, *21*, 1356. b) F. Helmchen, W. Denk, *Nat. Methods* **2005**, *2*, 932. c) F. Thorp-Greenwood, R. G. Balasingham, M. P. Coogan, *J. Organomet. Chem.* **2012**, *714*, 12.

[19] N. A. Dudina, A. Y. Nikonova, Y. V. Antina, M. B. Berezin, A. L. Vyugin, *Chem. Heterocycl. Compd.* **2014**, *29*, 1740.

[20] I. A. Karpenki, Y. Niko, V. P. Yakubovskyi, A. O. Gerasov, D. Bonnet, Y. P. Kovtunc, A. S. Klymchenko, *J. Mater. Chem. C* **2016**, *4*, 3002.

[21] M. Yu, C. Zhou, J. Liu, J. D. Hankins, J. Zheng, *J. Am. Chem. Soc.* **2011**, *133*, 11014.

[22] J. Han, K. Burgess, *Chem. Rev.* **2010**, *110*, 2709.

[23] Z. Yang, J. Cao, Y. He, J. H. Yang, T. Kim, X. Peng, J. S. Kim, *Chem. Soc. Rev.* **2014**, *43*, 4563.

[24] L. E. Shimolina, M. A. Izquierdo, I. López-Duarte, J. A. Bull, M. V. Shirmanova, L. G. Klapshina, E. V. Zagaynova, M. K. Kuimova, *Sci. Rep.* **2017**, *7*, 41097.

[25] H. Kobayashi, M. Ogawa, R. Alford, P. L. Choyke, Y. Urano, *Chem. Rev.* **2010**, *110*, 2620.

[26] O. S. Wolfeis, *Chem. Soc. Rev.* **2015**, *44*, 4743.

[27] a) E. Xochitiotzi-Flores, A. Jiménez-Sánchez, H. García-Ortega, N. Sánchez-Puig, M. Romero-Ávila, R. Santillan, N. Farfán, *New J. Chem.* **2016**, *40*, 4500.

[28] D. Su, C. L. Teoh, N. Gao, Q. H. Xu, Y. T. Chang, *Sensors* **2016**, *16*, 1397.

[29] **V-VI**J. Shanmugapriya, K. Rajaguru, G. Sivaraman, S. Muthusubramanian, N. Bhuvanesh, *RSC Adv.* **2016**, *6*, 85838. VII: W. Chen, L. Zhu, Y. Hao, X. Yue, J. Gai a, Q. Xiao, S. Huang, J. Sheng, X. Song, *Tetrahedron.* **2017**, *73*, 4529. **VIII-IX**: S. Chen, R. Qiu, Q. Yu, X. Zhang, M. Wei, Z. Dai, *Tetrahedron Lett.* **2018**, *59*, 2671.

[30] M. Ibarra-Rodríguez, B. M. Muñoz-Flores, H. V. R. Dias, M. Sánchez, A. Gómez-Treviño, R. Santillán, N. Farfán, V. M. Jiménez-Pérez, *J. Org. Chem.* **2017**, *82*, 2375.

[31] **L1**Y. Qiao, X. Ju, Z. Gao, L. Kong, *Acta Cryst. Sect. E* **2010**, *66*, o95. **L2**: C. Ji-Chun, P. Qian-Xiu, Y. Han-Dong, Q. Yan-Ling, *Acta Cryst. Sect. E.* **2007**, *63*, o2633

[32] L. Krause, R. Herbst-Irmer, G. M. Sheldrick, D. Stalke, *J. Appl. Crystallogr.* **2015**, *48*, 3.

[33] G. Sheldrick, *Acta Crystallogr. Sect. A: Found. Adv.* **2015**, *71*, 3.

[34] O. V. Dolomanov, L. J. Bourhis, R. J. Gildea, J. A. K. Howard, H. Puschmann, *J. Appl. Crystallogr.* **2009**, *42*, 339.

[35] G. M. Sheldrick, *Acta Cryst. Sect. A.* **2008**, *64*, 112.

[36] A. T. R. Williams, S. A. Winfield, J. N. Miller, *Analyst* **1983**, *108*, 1067.

[37] M. J. Frisch, G. W. Trucks, H. B. Schlegel, G. E. Scuseria, M. A. Robb, J. R. Cheeseman, G. Scalmani, V. Barone, B. Mennucci, G. A. Petersson, H. Nakatsuji, M. Caricato, X. Li, H. P. Hratchian, A. F. Izmaylov, J. Bloino, G. Zheng, J. L. Sonnenberg, M. Hada, M. Ehara, K. Toyota, R. Fukuda, J. Hasegawa, M. Ishida, T. Nakajima, Y. Honda, O. Kitao, H. Nakai, T. Vreven, J. A. Montgomery Jr., J. E. Peralta, F. Ogliaro, M. Bearpark, J. J. Heyd, E. Brothers, K. N. Kudin, V. N. Staroverov, R. Kobayashi, J. Normand, K. Raghavachari, A. Rendell, J. C. Burant, S. S. Iyengar, J. Tomasi, M. Cossi, N. Rega, M. J. Millam, M. Klene, J. E. Knox, J. B. Cross, V. Bakken, C. Adamo, J. Jaramillo, R. Gomperts, R. E. Stratmann, O. Yazyev, A. J. Austin, R. Cammi, C. Pomelli, J. W. Ochterski, R. L. Martin, K. Morokuma, V. G. Zakrzewski, G. A. Voth, P. Salvador, J. J. Dannenberg, S. Dapprich, A. D. Daniels, Ö. Farkas, J. B. Foresman, J. V. Ortiz, J. Cioslowski, D. J. Fox, *Gaussian 09, Revision B.01*, Gaussian, Inc., Wallingford CT **2009**.

[38] G. A. Petersson, M. A. Al-Laham, *J. Chem. Phys.* **1991**, *94*, 6081.

[39] a) F. Kaiser, J. White, C. Hutton, *J. Am. Chem. Soc.* **2008**, *130*, 16450. b) V. Barba, J. Vazquez, F. López, R. Santillán, N. Farfán, *J. Organomet. Chem.* **2005**, *690*, 2351. c) H. Nöth, B. Wrackmeyer, *Nuclear Magnetic Resonance Spectroscopy of Boron Compounds*, Springer-Verlag, New York **1978**.

[40] H. Hpfl, *J. Organomet. Chem.* **1999**, *581*, 129.

[41] K. Luby-Phelps, *Int. Rev. Cytol.* **1999**, *192*, 189.

[42] M. A. Haidekker, E. A. Theodorakis, *Org. Biomol. Chem.* **2007**, *5*, 1669.

[43] T. Frster, G. Z. Hoffmann, *Phys. Chem.* **1971**, *75*, 63.

[44] V. M. Jiménez-Pérez, M. C. García-López, B. M. Muñoz-Flores, R. Chan-Navarro, J. C. Berrones-Reyes, H. V. Rasika Dias, I. Moggio, E. Arias, J. A. Serrano-Mireles, A. Chávez Reyes, *J. Mater. Chem. B* **2015**, *3*, 5731.

[45] a) M. F. Santos, J. N. Rosa, N. R. Candeias, C. P. Carvalho, I. Matos, E. Ventura, F. Florindo, C. Silva, U. Pischel, M. P. Goi, *Chem. – Eur. J.* **2016**, *22*, 1631. b) Y. Zhou, Y. -Z. Chen, J. Hua Cao, Q. Zheng Yang, L. Zhu Wu, C. Ho Tung, D. Yong Wu, *Dyes Pigm.* **2015**, *112*, 162. c) M. Courtis, A. Santos, Y. Guan, J. A. Hendricks, B. Ghosh, D. M. Szantai-Kis, A. Reis, V. Shah, R. Mazitschek, *Bioconjugate Chem.* **2014**, *25*, 1043.

## SUPPORTING INFORMATION

Additional supporting information may be found online in the Supporting Information section at the end of the article.